J. Mt. Sci. (2018) 15(12): 2721-2729 e-mail: jms@imde.ac.cn http://jms.imde.ac.cn
https://doi.org/10.1007/s11629-018-5114-z

A debris-flow impact pressure model combining material characteristics and flow dynamic parameters

TANG Jin-bo http://orcid.org/0000-0002-7192-1224; e-mail: jinbotang@imde.ac.cn

HU Kai-heng* http://orcid.org/0000-0001-8114-5743; e-mail: khhu@imde.ac.cn

**Corresponding author*

Key Laboratory of Mountain Hazards and Surface Process, Chinese Academy of Sciences, Chengdu 610041, China; Institute of Mountain Hazards and Environment, Chinese Academy of Sciences, Chengdu 610041, China

Citation: Tang JB, Hu KH (2018) A debris-flow impact pressure model combining material characteristics and flow dynamic parameters. Journal of Mountain Science 15(12). https://doi.org/10.1007/s11629-018-5114-z

Abstract: Impact force is a crucial factor to be considered in debris-resisting structure design. The impact of debris flow against a structural barrier depends not only on the flow dynamics but also on the barrier material. Based on the structural vibration equation and energy conservation law, a simple model for calculating debris-flow impact pressure is proposed, which includes the mechanical impedance of the material, debris-flow velocity and Froude number. Twenty-five impact tests have been conducted using different kinds of materials: steel, black granite, white granite, marble and polyvinyl chloride (PVC) board, and the ratio of the maximum impact time to the vibration period of the structure is determined for the model. It is found that the ratio's square root shows a linear relationship with the material solid Froude number. This indicates that the impedance of the structures plays an important role in the flow-barrier interaction. Moreover, the debris-flow impact force is found to decrease with the travel time of the elastic stress wave though the structures.

Keywords: Debris flows; Impact pressure; Dynamical responses; Mechanical impedance

Introduction

Debris flows are common type of geological hazards that can be viewed as an intermediate form of mass movement between hyper-concentrated flows and landslides (Iverson 1997). When the debris flows encounter structures, since debris flows have greater kinetic energy, the great impact force acting on the structures can result in structural damage, even to extent of causing a natural disaster. Therefore, determinations of the impact force of debris flows can play an important role in the design of prevention engineering.

Recently, based on field measurements (Okuda et al. 1977; Zhang 1993; Hu et al. 2006; König et al. 2006; Wendeler et al. 2007; Hu et al. 2011) and scale experiments (Wei 1996; Armanini 1997; Liu et al. 1997; Shieh et al. 2008; Yang et al. 2011; Scheidal et al. 2012; Song et al. 2017), the impact force of debris flows have been widely investigated. In these studies, debris flows were usually viewed as heterogeneous two-phase flows, composed of a liquid-phase slurry and solid-phase grains (Iverson 1997). Correspondingly, the impact forces of debris flows have been described as the sum of the slurry impact pressure and grain impact loading (Mitsuyama 1979; Zhang 1993; Chen and Tang 2006; Hübl et al. 2009; Hu et al. 2011; Lei et al. 2017). Meanwhile, the slurry impact pressure investigations can be divided into two types, namely, those involving hydrostatic models and those involving hydrodynamic modeling (Lichtenhahn 1973; Watanabe and Ike 1981; Zhang 1993; Armanini 1997; Zanchetta et al. 2004; Egli 2005; Bugnion et al. 2011; Proske et al. 2011; Cui et al. 2015). On the other hand, the determinations of the impact loading of solid-phase grains including

Received: 09 July 2018
Revised: 26 October 2018
Accepted: 01 November 2018

boulders have been typically carried out with methods of solid mechanics, such as through the application of the Hertz law (Huang et al. 2007; He et al. 2009; Cui et al. 2018), theory of cantilever beam (Wang et al. 2009) and single degree of freedom model of collision (Haehnel and Daly 2004).

Presently, the determinations of the critical particle size between solid and fluid phases are necessary but remain unresolved when debris flows are viewed as two-phase flows (Yang et al. 2014). An alternative model is the mixture fluid model that has been used to describe the dynamical process of debris flows (Iverson and Delinger 2001). Odo (1994) argued that debris flows can be viewed as a kind of compressible mixture fluid and established a dynamical model for debris flows. Based on that work, Wei (1996) pointed out that the impact forces of debris flows are mainly derived from the propagation of pressure wave in fluids. Liu et al. (1997) proposed that debris flows can be described as Bingham fluids and established a determining method for debris flows impact pressure based on the mass equation and momentum equation.

In regard to the mixture fluid models, although the dynamical properties of debris flow have been considered for determination of the impact forces of debris flows, the effects of the mechanical properties of structural materials and shapes on impact force are rarely studied (Tan et al. 2017; Yu et al. 2017). Shieh et al. (2008) argued that the shape of Sabo dams has significant influence on the impact force of debris flows and pointed out that the impact force of debris flows for a curved dam would be smaller than that for a vertical dam and slanted dam based on flume experiments. However, the impacted structures in these models were assumed as absolutely rigid bodies. Although debris flows are viewed as the mixture fluids, numerous pebbles and even boulders, whose mechanical properties are similar to structures' materials, are present during the motion of debris flows (Cui et al. 2005). Therefore, the effects of the mechanical properties of structural materials should not be ignored when investigating the impact force of debris flows.

In this study, debris flows were viewed as a mixture fluid and the mechanical properties of structural material were considered when determining the impact force of debris flows. Furthermore, the dynamical responses of structures made with different materials to the impact force of debris flows were studied. A simple debris-flow impact model was derived based on the principle of energy conservation and on the no-damping single degree of freedom model of collision in this study. The influence of the mechanical parameters of structures impacted by debris flows, including that of the elasticity modulus and density was studied by flume experiments. By comparing the experimental results with the theoretical model, a correction coefficient incorporating the effects of material parameters was determined and taken account into the model.

1 Research Method

1.1 A simplified model of dynamical responses to debris-flow impact

Following Iverson's mixture model (Iverson and Denlinger 2001), debris flows can viewed as the fluid mixture consisting of a liquid-phase slurry and solid-phase grains. During motion, debris flows take great kinetic energies. When debris flows encounter the structures, an enormous impact force acts on the surface of structures and this may lead to the structural damage. Conversely, the presence of structures can affect the motion of debris flows (Nakatani et al. 2013). Because numerous grains, pebbles, and even boulders impact the structures, during the interaction between debris flows and structures, the structures should not be assumed as the rigid body. Therefore, the structures have dynamical responses to impacts generated by debris flows. To illustrate the dynamical responses of structures impacted by debris flows, the following simplified vibrating model, which is based on the structural dynamics (Clough and Penzien 1993), is proposed:

$$m\frac{d^2x}{dt^2}+kx=P(t) \tag{1}$$

where x is the vibration displacement of the structure; $m=BHl\rho_b$ is the mass of the structure; B, l and H are the width, thickness and height of structure, respectively; t is the time; $k=EA/l$ is the stiffness coefficient of the material, E is the elastic modulus of structural material, $A=BH$ is the whole area of structures surface that suffered from debris flows; ρ_b is the density of the structure; and $P(t)$ is the real-time impact force of debris flows.

Suppose that the structure achieved maximum vibration displacement $x_{max}=s$ in the time Δt when the structure was impacted. According to the theory of structural dynamics (Clough and Penzien 1993), the natural period of vibration of the structure is $T=2\pi\sqrt{m/k}$. For a free vibration state, Δt is equal to $T/4$. However, for general forced vibration, Δt hasn't analytical expression because of uncertainty of $P(t)$ in Eq. (1). For simplicity, we set Δt is equal to λT, where λ depends on the mechanical properties of structural material and dynamical properties of debris flows. During the process, the moving distance of debris flows is the product of the velocity of debris flows and the time Δt.

The velocity of debris flows is assumed to have vanished after the structures were impacted. Therefore, during the time Δt, the mass of debris flows impacting the structures can be formulated as

$$M_d = \Delta t \rho_d Bhv = 2\pi\lambda\sqrt{\frac{m}{k}}\rho_d Bhv \qquad (2)$$

where ρ_d, h, v are respectively the density, height and velocity of debris flows.

Furthermore, the kinetic energy of debris flows, during the time Δt, is assumed to be fully translated into the elastic energy of the structure. During the process, inelastic deformations are absent in the structures. And in the time Δt, the maximum vibration displacement s is present in the structures.

According to the principle of the conservation of energy, the kinetic energy of debris flows during the time period of analysis is equal to the maximum elastic energy of the structure, as follows

$$\frac{1}{2}M_d v^2 = \frac{1}{2}ks^2 \qquad (3)$$

By substituting Eq.(2) into Eq.(3), the maximum vibration displacement of the structure can be written as follows:

$$s = \sqrt{\frac{2\pi\lambda}{EA}\sqrt{\frac{ml}{EA}}\rho_d Blhv^3} \qquad (4)$$

Now, maximum impact force acting on the structures is obtained as follows:

$$F_m = ks = \sqrt{2\pi\lambda\rho_d B^2 Hhv^3\sqrt{\rho_b E}} \qquad (5)$$

Meanwhile, the area of interaction between structures and debris flows is $A_s=Bh$. If the height of debris flows h is greater than the height of structures H, let $A_s=BH$. In other words, $A_s=Bh_s=B\min(h,H)$, where $h_s=\min(h,H)$ represents the minimum value between h and H. Therefore, the impact pressure of the debris flows can be expressed by:

$$P_c = \frac{F_m}{Bh_s} = \sqrt{\frac{H}{h_s}2\pi\lambda\rho_d v^3\sqrt{\rho_b E}} \qquad (6)$$

A solid Froude number α is introduced in this study, which is similar to the fluid Froude number in fluid mechanics:

$$\alpha = \frac{c_b}{\sqrt{gH}} \qquad (7)$$

where g is the acceleration of gravity, $c_b=\sqrt{E/\rho_b}$ represents the velocity of the elastic stress wave of structures (Yu et al. 2011), α can be explained as the reciprocal of the dimensionless time that elastic stress wave moved though the structures .

Finally, Eq. (6) can be simplified together with Eq. (7) as follows:

$$P_c = \sqrt{2\pi\lambda}\frac{Fr}{\alpha}c_b\sqrt{\rho_d v\rho_b c_b} \qquad (8)$$

In Eq. (8), $\rho_b c_b=\sqrt{\rho_b E}$ is the mechanical impedance of the structural materials which represents the level of resistance to deformation of materials (Yu et al. 2011), and $Fr=\sqrt{v/gh_s}$ is the Froude number of the debris flows (Iverson 1997).

1.2 Flume experiments

Because an unknown parameter λ is present in Eq.(8), flume experiments were conducted in this study to determine the impact pressure of debris flows. The experimental setup in this study is mainly consisted of column storage hopper, flume and tailings pond (as shown in Figure 1). The edges and height of column storage hopper were 1 m and 1 m respectively. The flume was 3 m long and 0.4 m wide. The flume slope of the flume was fixed at 20% in order to reduce the effect of the slope of the flume on the impact pressure.

The bottom of the flume was marked by several black lines every 0.2 m, which were used to determine the velocity of the front of debris flows by a camera that can record 25 frames per second. The flowing depth of debris flows was measured directly by a laser distance sensor installed at a vertical distance of 0.5 m above the flume bed as shown in Figure 1. The laser sensor recorded 10 data points per second. The data acquisition system for recording the impact pressure of debris flows includes data acquisition instrument with sampling frequency of 2000 Hz, signal amplifier and computer (Figure 2). In our experiments, each pressure sensor had sensitivity of 1.5±0.1 Pa/kPa, and a forced surface with a 2 cm diameter (Figure 3).

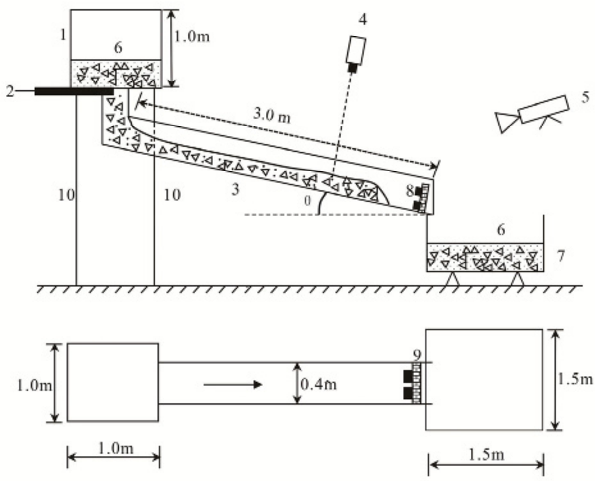

Figure 1 Lateral and vertical view of experiments in this study and corresponding geometric scales (In detail, 1. Debris flows hopper; 2. Sluice gate used to release debris flows; 3. Flume stabled slope θ with 20%; 4. Laser sensor; 5. Camera used to record the flowing process; 6. Debris flows in tailing pool; 7. Tailing pool; 8. Pressure sensors; 9. Rectangle structure used to install impact sensor; 10. Steel frame used to support the debris flows hopper)

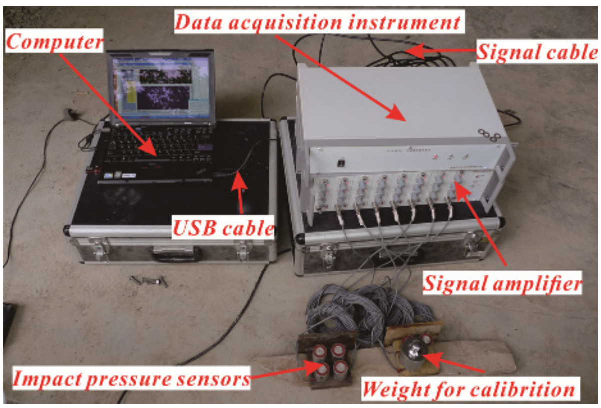

Figure 2 Debris-flow impact pressure measurement system consisting of computer, data acquisition instrument, signal amplifier, impact pressure sensors, signal cable and USB cable.

Five kinds of rectangular boards were fitted with installed pressure sensors (Figure 1). These boards were made of different materials including steel, marble, black granite and white granite, PVC (polyvinyl chloride) materials, and were used to study the dynamical responses of different materials to impacts generated by debris flows. Some mechanical properties of these materials, which were obtained through the literatures (Goodman 1989; Chizhik et al. 1998; Li et al. 2005; Martel 2005), and the height of the structures are shown in Table 1.

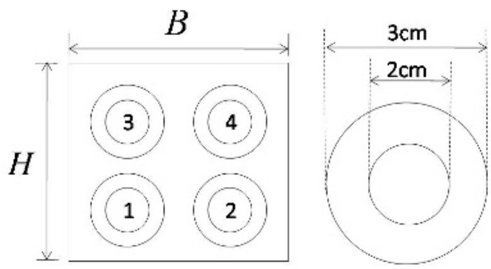

Figure 3 The distribution of impact pressure sensors for experiments (The four sensors are installed into four holes numbered 1, 2, 3, 4).

Table 1 The height and material parameters of structures in the experiments

Material	H (cm)	E (10^9Pa)	D (kg/m^3)	α (10^3)
Steel	10.0	206	7800	5.1912
Black granite	10.0	60	2730	4.8048
White granite	10.0	48	2600	4.2778
Hard PVC board	10.0	4	1400	1.7074
Marble	10.0	55	2700	4.5592

Notes: H–Height, E–Elastic modulus and D–Density of structures.

Soil materials were derived from deposits on the fan of debris flows in Jiangjia Gully, which is located in Dongchuan city, Yunnan Province, China (Cui et al. 2005). In order to avoid the effect of compositions of soil on the impact pressure of debris flows, just one soil composition was used to conduct the experiments in this study. The particle grading curve of soil materials in our experiments is shown in Figure 4. The maximum grain size d_{max} of experimental soil was 2 cm and the width B_f (=0.4 m) of flume satisfied the control boundary condition $B_f \geq d_{max}$ (Chen et al. 2018).

During the experiments, debris flows with a volume of 0.3 m^3 of poorly water-saturated mixtures of sands and gravels were set to move at a steady state after a traveling distance of 2 m from the upper part of the flume. In most cases, the whole flowing process lasted about 10 seconds according to the results from the laser meter

(Figure 5). The structures impacted by debris flows were installed with a central line distance of 2.8 m from the storage hopper to ensure that debris flows were moving steadily before impacting the structures and that the impacts occurred vertically on the four pressure sensors installed on the surface of the structures. For each kind of structural materials, five experiments were conducted. The density of debris flows for each experiment could be measured directly by a sampling beaker and electronic balance (Table 2). The front velocity of debris flows was calculated by combining the movement distance of debris flows front in the flume bed with the movement time recorded by video (the data are listed in Table 2). The depth of debris flows front could be measured by laser sensor (see Table 2).

For signals of the impact pressure of debris flows, however, whether derived from field monitoring or flume experiments, the recorded signals always contain noise (Hu et al. 2011; Tang et al. 2013). Therefore, the measured impact signals of debris flow were de-noised first based on a Db4 wavelet analysis to obtain the realistic impact signals (shown in Figure 6). These impact signals showed that the front part of debris flows had a stronger impact force than the middle and tail parts. A possible explanation for this is the density and velocity of debris flows surge's front are larger than other parts of debris flows (Iverson 1997). The maximum impact force in the front parts of debris flows may be, in most cases, the main cause of the failure of the structures and is utmost important concern for the design of mitigation measures. The maximum values of de-noised impact force signal were picked out for subsequent analysis.

$$P = \max_{1\le i\le 4} \max_{1\le k\le n} (P_i(k)) \tag{9}$$

where $P_i(k)$ is the time series of de-noised signal recorded by sensor number i (i = 1, 2, 3, 4) in Figure 6. P is the maximum impact pressure of de-noised signals, n is the number of time series of impact signals.

For each experiment, the maximum impact pressure P of the de-noised signal was extracted based on Eq.(9) and the results are listed in Table 2. According to Table 2, the impact pressures were not only dependent on the magnitude of flow depth, density and velocity, but also were related to the type of material in the structure. Especially, the measured impact pressures for the PVC board (<100 kPa) appeared to be smaller than other four kinds of materials.

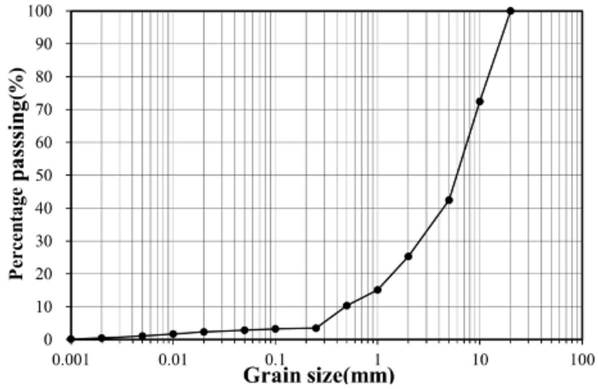

Figure 4 Particle size distributions of soil materials in this study.

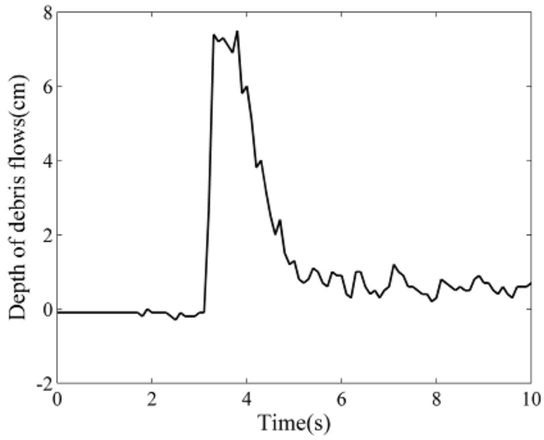

Figure 5 An example (H-2, as listed in Table 2) of the time series of the depth of debris flows with hard polyvinyl chloride (PVC) board during the experiments.

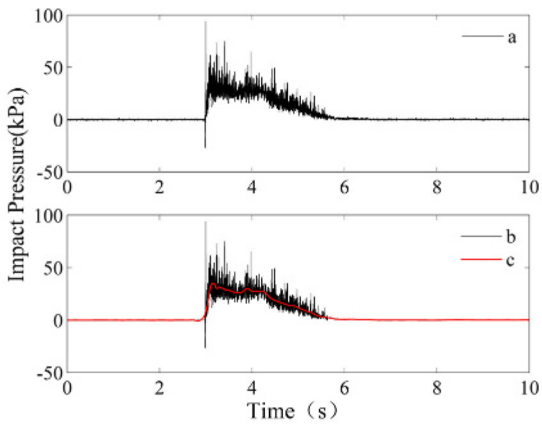

Figure 6 An example (H-2, as listed in Table 2) of the time series of measured (a), de-noised (b) and smoothed signal of impact force (c) of debris flows with hard polyvinyl chloride (PVC) board during the experiments.

2 Results and Discussion

In Eq.(8), the parameter λ is an unknown parameter, as previously mentioned. In this study, λ was assumed to only depend on the mechanical properties of structural material, since differences in mechanical properties of soil materials were absent. To illustrate the influence of the mechanical properties of structural material on impact pressures of debris flows, a dimensionless parameter β is introduced as

$$\beta = \sqrt{\lambda} = \frac{P_c}{P_m} \quad (10)$$

where P_c is as described in Eq.(8), P_m can be described as follows:

$$P_m = \sqrt{2\pi}\,\frac{Fr}{\alpha} c_b \sqrt{\rho_d v \rho_b c_b} \quad (11)$$

By substituting the corresponding measured data in Table 2 into Eq.(8), for each flume experiment, the value of β was calculated, and the results are shown in Figure 7. The results showed that the values of β are different for the five structural materials. The different values of β or λ indicate that the different structures will have different dynamical responses to impacts generated by debris flows.

Since marble, white granite and black granite are heterogeneous material (Goodman 1989), impact pressures corresponding to these material were scattered (Figure 7). Meanwhile, the steel and PVC boards were man-made and more homogeneous compared with the other rock-based materials; consequently, the impact pressures of steel and PVC boards were more centralized (Figure 7). Furthermore, five linear empirical relationships between the measured impact pressure P in the experiment and impact pressure P_m calculated by Eq.(11) were proposed for the five structural materials and these are shown in Figure 8.

According to the results in Figure 8, the values of β for structures made of steel, black granite, white granite, marble and polyvinyl chloride (PVC) board are 0.0222, 0.0362, 0.0409, 0.0401 and 0.0782, respectively. And the largest value of β was equal to 0.0782 for the PVC material, while the smallest one was 0.0222 for the steel material. For five structural materials selected in our study, the mechanical impedance of the PVC material was the smallest and was equal to 2.36×10^6 m/s. Meanwhile for steel material, the mechanical impedance was largest and was equal to 40.08×10^6 m/s. In other words, the findings indicate that the structures made of PVC material are more easily deformable and will take a longer time to reach greater

Table 2 The measured velocity, flowing depth, density and de-noised impact force of debris flow front

Material	v (m/s)	h (m)	D_d (g/cm^3)	P (kPa)
S-1	3.16	0.100	1.9329	84.1426
S-2	3.75	0.101	2.0000	113.2202
S-3	3.33	0.071	2.0164	112.2695
S-4	4.00	0.078	2.0445	145.0008
S-5	4.00	0.087	1.9871	139.0585
B-1	4.29	0.090	2.1270	134.2617
B-2	4.29	0.080	2.0434	139.3785
B-3	4.00	0.082	2.1051	120.9000
B-4	4.00	0.075	2.1195	139.6011
B-5	4.00	0.079	2.0683	134.9257
W-1	3.75	0.075	2.1751	152.2300
W-2	3.53	0.067	2.2321	114.1387
W-3	4.00	0.073	2.1452	152.0308
W-4	3.53	0.072	2.1812	145.9306
W-5	3.53	0.069	2.1218	111.1158
H-1	3.53	0.069	2.1290	120.2483
H-2	3.33	0.072	2.0616	92.0953
H-3	3.16	0.071	2.0479	90.3997
H-4	3.00	0.074	2.1526	82.6571
H-5	3.16	0.067	2.1240	94.5280
M-1	3.53	0.075	2.2617	134.0878
M-2	3.33	0.066	2.0723	113.0451
M-3	3.33	0.073	2.1376	113.7925
M-4	3.16	0.071	2.0028	107.7576
M-5	3.00	0.069	2.1675	101.6434

Notes: S-Steel, B-Black granite, W-White granite, H-Hard polyvinyl chloride (PVC) board, M-Marble, v-the velocity of debris flow front, h-The depth of debris flow front, D_d-density of debris flow, P-de-noised impact force.

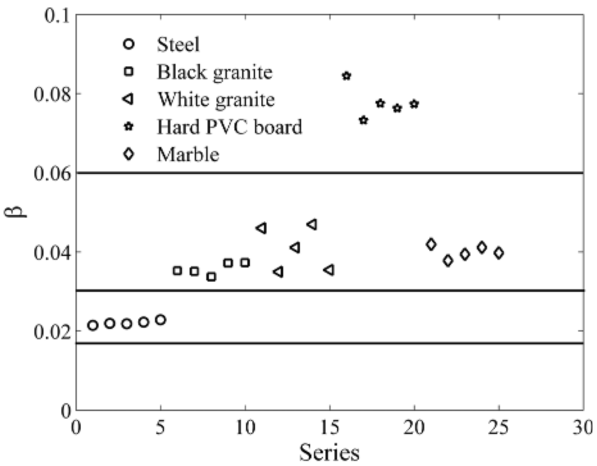

Figure 7 The value of the dimensionless parameter β as formulated in Eq. (10) for five structural materials made of steel, black granite, white granite, marble and polyvinyl chloride (PVC) board.

deformation, compared to the other structural materials in our study (vice versa, for steel material).

By comparing the values of the parameters in Table 1 and the β data shown in Figure 7, it was discovered that the white and black granite materials had a similar value of α and β, and a trend was detected in which larger the values of α were associated with smaller values of β. The negative linear relevant relation between α and β is shown in Figure 9. This relationship was fitted as follows,

$$\beta = -1.4780\times10^{-5}\alpha + 0.1045 \quad (12)$$

where the fitting correlation coefficient (R^2) was 0.9651.

By substituting Eq.(12) into Eq.(8), the calculation formula for the impact pressure of debris flows can be formulated as follows:

$$P_c = (-3.7039\times10^{-5} + \frac{0.2618}{\alpha}) Frc_b\sqrt{\rho_d v \rho_b c_b} \quad (13)$$

The relationship between the measured impact pressures and those estimated with Eq. (13) are shown in Figure 10.

According to Eq. (13), the impact pressure of debris flows acting on a structure is caused by the interaction between the debris flows and the structure. The dynamical parameters of debris flows and the mechanical properties of structural materials both play an important role in the dynamical responses of structure impacted by debris flows. However, in previous studies on the impact pressure of debris flows, structures have been usually viewed as the rigid bodies and the influence of mechanical properties of structural materials on the impact pressure of debris flows has been ignored. In these studies, the hydrodynamic pressure was usually modified to determine the impact pressure of debris flows (Kang et al. 2004), e.g.

$$P = k\rho v^2 \quad (14)$$

where k is an empirical coefficient that ranges from 2.0 to 4.0 (Kang et al. 2004). By fitting Eq. (14) based on the experimental data in this study, we obtained k=4.31 (R^2=0.5046). For the modified hydrodynamic pressure, the root mean square error ($RMSE = \sqrt{\sum_{i=1}^{N}(P_{meas,i} - P_{model,i})^2 / N}$) and the maximum relative error ($MRE = \max_{1\le i\le n}[(P_{meas,i} - P_{model,i})/P]\times100\%$) were 14.68

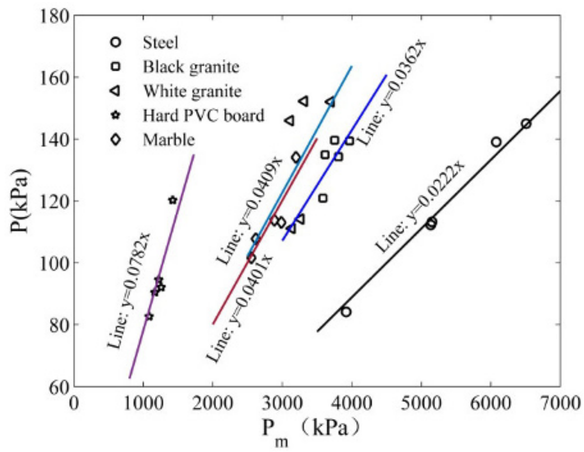

Figure 8 The relationship between measured impact pressure P and the calculated impact pressure Pm by Eq.(11) for five structural materials made of steel, black granite, white granite, marble and polyvinyl chloride (PVC) board. And the five lines have different slopes, which represent different values of β.

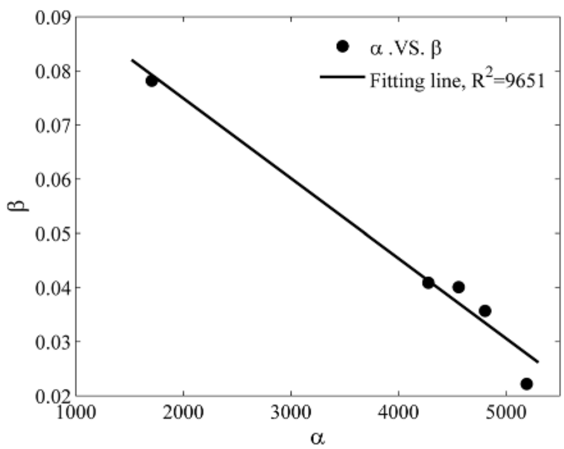

Figure 9 The negative relationship between the solid Froude number α as formulated in Eq. (7) and the dimensionless parameter β as formulated in Eq. (10).

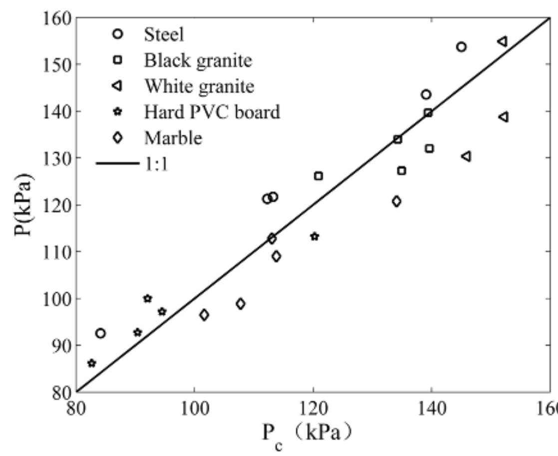

Figure 10 The relation of the measured and calculated impact pressures with Eq. (13).

kPa and 25.66%, respectively. Here $P_{meas,i}$ and $P_{model,i}$ were separately measured impact pressure of debris flow and calculated those, and N represents the total number of experiments. For the model proposed in this study, the root mean square error and the maximum relative error were 9.48 kPa and 19.71%, respectively. These results means that the model proposed in this study is more reliable than the model of modified hydrodynamic pressure.

3 Conclusions

In this study, the effects of mechanical properties of structural materials on the impact pressure of debris flows were examined. The following conclusions were drawn:

(1) The results showed that mechanical properties of the structural materials played an important role in determining the impact pressure of debris flows. The impact pressure of debris flows is thus dependent on both the dynamical properties of debris flow and the mechanical properties of structural materials.

(2) In this study, a method for the determination of the impact pressure of debris flow was proposed based on a simplified dynamical response model of structures impacted by debris flows and was modified based on the experimental data for five structural materials including steel, black granite, white granite, marble and PVC board. The calculation formula of debris flows impact pressures can be proposed as follows:

$$P_c = (-3.7039\times10^{-5} + \frac{0.2618}{\alpha})Frc_b\sqrt{\rho_d v \rho_b c_b}$$

(3) A smaller mechanical impedance implies that a structural material can be more easily deformed. For structural material with small mechanical impedance, the time that elastic stress wave passes though the structure is longer and the impact pressure caused by debris flows is smaller than the corresponding value for structural material with large mechanical impedance. Therefore, under the premise of ensuring strength, the use of flexible materials can reduce the impact pressure of debris flows.

Acknowledgments

This work has been supported by the National Natural Science Foundation of China (Grant No. 41601011), National Natural Science Foundation of China (Grant No. 41790434) and National Natural Science Foundation of China (41771045).

Reference

Armanini A (1997) On the dynamic impact of debris flows. In: Armanini A and Masanori M (eds), Recent Developments on Debris Flows, Lecture Notes in Earth Sciences, Springer, Berlin. pp 208-226.

Bugnion L, McArdell B, Bartelt P and Wendeler C (2012) Measurements of hillslope debris flows impact pressure on obstacles. Landslides 9(2) 179-187. https://doi.org/10.1007/s10346-011-0294-4

Chen H and Tang H (2006) Method to calculate impact force and impact time of two-phase debris flows. China Journal of Highway and Transport 19(1): 19-23. (In Chinese) https://doi.org/10.19721/j.cnki.1001-7372.2006.03.004

Chen JG, Chen XQ, Zhao WY, and You Y (2018) Debris flow drainage channel with energy dissipation structures: experimental study and engineering application. Journal of Hydraulic Engineering 144(10): 06018012. https://doi.org/10.1061/(ASCE)HY.1943-7900.0001523

Chizhik SA, Huang Z, Gorbunov VV, et al. (1998) Micromechnical properties of elastic Polymetric material as probed by scanning force microscopy. Langmuir 14(8): 2606-2609. https://doi.org/10.1021/la980042p

Clough RW and Penzien J (1993) Dynamics of Structures. McGraw-Hill, New York.

Cui P, Chen XQ, Wang Y, et al. (2005) Jiangjia Ravine debris flows in south-western China. In: Jackob M and Hungr O (eds), Debris-flow Hazards and Related Phenomena. Praxis, Springer Berlin Heidelberg. pp 565-594. https://doi.org/10.1007/3-540-27129-5_22

Cui P, Zeng C, Lei Y (2015) Experimental analysis on the impact force of viscous debris flow. Earth Surface Processes and Landforms 40(12): 1644-1655. https://doi.org/10.1002/esp.3744

Cui YF, Choi CE, Liu LHD, Ng CWW (2018) Effects of particle size of mono-disperse granular flows impacting a rigid barrier. Natural Hazards 91(3): 1179-1201. https://doi.org/10.1007/s11069-018-3185-3

Egli T (2005) Guide, object protection against gravitative Natural hazards. Association of Cantonal Fire Insurance (VKF). (In Germany)

Goodman RE (1989) Introduction to Rock Mechanics. 2nd ed, New York, John Wiley & Sons.

Haehnel RB and Daly SF (2004) Maximum impact of woody debris on floodplain structures. Journal of Hydraulic Engineering 130(2): 112-120. https://doi.org/10.1061/(ASCE)0733-9429(2004)130:2(112)

He S, Wu Y, Shen J (2009) Simplified calculation of impact force of massive stone in debris flows. Journal of Natural Disaster 18(3): 51-56. (In Chinese) https://doi.org/10.13577/j.jnd.2009.0508

Hu KH, Wei FQ, Hong Y, Li XY (2006) Field measurement of

impact force of debris flows. Chinese Journal of Rock Mechanics and Engineering 25: 2813-2819. (In Chinese)
Hu KH, Wei FQ, Li Y (2011) Real-time measurement and preliminary analysis of debris-flow impact force at Jiangjia ravine, China. Earth Surf Process Landforms 36: 1268-1278. https://doi.org/10.1002/esp.2155
Huang HP, Yang KC, Lai SW (2007) Impact force of debris flow on filter dam. Momentum 9(2): 03218. https://doi.org/10.1.1.601.135
Hübl J, Holzinger G (2003) Development of fundamentals for Dimensioning of crown-open structures for the Geschiebebewirtschaftung in torrents: Small scale model try to the effect of Murbrechern. WLS report 50 Volume 3, Institute of Mountain Risk Engineering. (In Germany)
Hübl J, Suda J, Proske D, et al. (2009) Debris flows impact estimation. In: Popovska C, Jovanovski M (eds.), Eleventh International Symposium on Water Management and Hydraulic Engineering 1: 137-148. https://www.researchgate.net/publication/258550978
Iverson RM (1997) The physics of debris flows. Reviews of geophysics 35(3): 245-296. https://doi.org/10.1029/97RG00426
Iverson RM and Denlinger RP (2001) Flow of variably fluidized granular masses across three-dimensional terrain. 1: Coulomb mixture theory. Journal of Geophysical Research 106(B1:537-552. https://doi.org/10.1029/2000JB900329
Kang ZC, Lee CF, et al. (2004) The Research of Debris Flow in China. Beijing: Science Press. (In Chinese)
König U (2006) Real scale debris flows tests in the Schesatobel valley. Master's thesis, University of Natural Resources and Life Sciences, Vienna, Austria.
Lei Y, Cui P, Zeng C and Guo YY (2017) An empirical mode decomposition-based signal process method for two-phase debris flow impact. Landslides 15(17). https://doi.org/10.1007/s10346-017-0864-1
Li J, Wei X, Li X and Qaing S (2005) Experiment of complex loading on the cash-steel joint of large steel-reticulated shell structure. China Civil Engineering Journal 38(4): 8-12. https://doi.org/10.15951/j.tmgcxb.2005.06.002
Lichtenhahn C (1973) Die Berechnung von Sperren in Beton und Eisenbeton. Kolloquium über Wildbachsperren, Mitteilungen der Forstlichen Bundesanstalt Wien 102: 91-127.
Liu KF, Lee FC and Tsai HP (1997) The flow field and impact force on a debris dam. In: Chen CL (ed.), Proceeding of the 1st International Conference on Debris-Flow Hazards Mitigation: Mechanics, Prediction and assessment, New York: ASCE. pp 737-746.
Martel S (2005) Special surface for power delivery to wireless micro-electro-mechanical systems. Journal of Micromechanics and Microengineering 15: S251-S258. https://doi.org/10.1088/0960-1317/15/10/S01
Mitsuyama T (1979) Evaluation of impact of debris flows on check dams. Journal of the Japan Society of Erosion Control Engineering 32(1): 40-49. (In Japanese)
Nakatani K, Okuyama Y, Hasegawa Y, et al. (2013) Influence of housing and urban development on debris flow flooding and deposition. Journal of Mountain Science 10(2): 273-280. https://doi.org/10.1007/s11629-013-2507-x
Odo J (1994) Study on debris flows impact force. Hydrotechnics Proceeding. p 38. (In Japanese)
Okuda S, Suwa H, Okunishi K, et al. (1977) Synthetic observation on debris flows, Part 3. Observation at Valley Kamikamihorizawa of Mt Yakedake in 1976. Annuals of Disaster Prevention Research Institute, Kyoto University 20B(1): 237-263. (In Japanese)
Proske D, Suda J and Hübl J (2011) Debris flows impact estimation for breakers. Georisk: Assessment and Management of Risk for Engineered Systems and Geohazards 5(2): 143-155. https: //doi.org/10.1080/17499518.2010.516227
Scheidl C, Chiari M, Kaitna R, et al. (2013) Analysing debris-flow impact models, based on a small scale modelling approach. Surveys in Geophysics 34(1): 121-140. https://doi.org/10.1007/s10712-012-9199-6.
Shieh CL, Ting CH, Pan HW (2008) Impulsive force of debris flows on a curved dam. International Journal of Sediment Research 23: 149-158. https://doi.org/10.1016/S1001-6279(08)60014-1
Song D, Ng CWW, Choi CE, et al. (2017) Influence of debris flow solid fraction on rigid barrier impact. Canadian Geotechnical Journal 54(10):1421-1434.https://doi.org/10.1139/cgj-2016-0502
Tan DY, Yin JH, Qin JQ, Zhu ZH (2017) New Thoughts for Impact Force Estimation on Flexible Barriers. In: Workshop on World Landslide Forum. Springer, Cham. pp 457-463. https://doi.org/ 10.1007/978-3-319-53483-1_54
Tang JB, Hu KH, Zhou GD, Chen HY (2013) Debris flows impact pressure signal processing by the wavelet analysis. Journal of Sichuan University (Engineering science edition) 45(1): 8-13. (In Chinese) https://doi.org/10.15961/j.jsuese.2013.01.003
Wang Q, He S and Zhang J (2009) Theoretical method for calculating impact force on debris flows protection piers. Journal of disaster Prevention and Mitigation Engineering 29(2): 423-427. (In Chinese) https://doi.org/10.13409/j.cnki.jdpme.2009.04.007
Watanabe M, Ikeya H (1981) Investigation and analysis of volcanic mud flows on mount sakurajima in Japan. In: Erosion sediment transport measurement. International Association on Hydrology, Florence, Science Publication 133: 245-256.
Wei H (1996) Experimental Study on impact force of debris flows heads. Chinese Railway Science 17(1): 50-61. (In Chinese)
Wendeler C, Volkwein A, Denk M, et al. (2007) Field measurements used for numerical modeling of flexible debris flows barriers. In: Chen C and Major J (eds.), Debris-Flow Hazards Mitigation Mechanics, Prediction and Assessment, Millpresss, Rotterdam.
Yang HJ, Wei FQ, Hu KH, et al. (2011) Measuring the Internal Velocity of Debris flowss Using Impact Pressure Detecting in the Flume Experiment. Journal of Mountain Science 8: 109-116. https://doi.org/10.1007/s11629-011-2083-x
Yang HJ, Wei FQ, Hu KH, Wang CC (2014) Determination of the suspension competence of debris flows based on particle size analysis. International Journal of Sediment Research 29(1): 73-81.https://doi.org/10.1016/S1001-6279(14)60023-8
Yu TX, Qiu XM (2011) Impact Dynamics. Beijing: Tsinghua University Press. (In Chinese)
Yu XB, Chen XQ (2017) Variational laws of debris flow impact force on the check dam surface based on orthogonal experiment design. Geotechnical and Geological Engineering 35(6):2511-2522.https://doi.org/10.1007/s10706-017-0258-0
Zanchetta G, Sulpizio R, Pareschi MT, et al. (2004) Characteristics of May 5-6,1998 volcaniclastic debris flows in sarno area (Campania, Southern Italy): Relationships to structure damage and harzard zonation. Journal of Volcanology and Geothermal Research 133: 377-393. https://doi.org/10.1016/S0377-0273(03)00409-8
Zanuttigh B, Lambberti A (2006) Experimental analysis of the impact of dry avalanches on structures and implication fordebris flows. Journal of Hydraulic Research 44(2): 522-534. https://doi.org/10.1080/00221686.2006.9521703
Zhang SC (1993) A comprehensive approach to the observation and prevention of debris flows in China. Natural Hazards 7: 1-23. https://doi.org/10.1007/BF00595676
Zhang Y, Wei FQ, Wang Q (2007) Experimental research of reinforced concrete buildings struck by debris flows in mountain areas of western China. Wuhan University Journal of Natural Sciences 12(2): 645-650. https://doi.org/10.1007/s11859-006-0339-z